Conference on Modelling Fluid Flow (CMFF'25)
The 19th International Conference on Fluid Flow Technologies
Budapest, Hungary, August 26-August 29, 2025

Flow Diverter Treatment For Intracranial Media Bifurcation Aneurysms: Challenging the Predictive Role of Morphology and Hemodynamics

Anna Bernovskis[1,8], Janneck Stahl[2,8], Gabor Janiga[3,8], Matthias Gawlitza[4], Daniel Behme[5,8], Philipp Berg[6,8], Samuel Voß[7,8]

[1] Corresponding Author. Department of Healthcare Telematics and Medical Engineering, University of Magdeburg, Universitätsplatz 2, 39106 Magdeburg, Germany. E-mail: anna.bernovskis@ovgu.de
[2] Department of Healthcare Telematics and Medical Engineering, University of Magdeburg, Universitätsplatz 2, 39106 Magdeburg, Germany. E-mail: janneck.stahl@ovgu.de
[3] Laboratory of Fluid Dynamics and Technical Flows, University of Magdeburg, Universitätsplatz 2, 39106 Magdeburg, Germany. E-mail: gabor.janiga@ovgu.de
[4] Department of Neuroradiology, University Clinic Jena, Am Klinikum 1, 07747 Jena, Germany. E-mail: matthias.gawlitza@med.uni-jena.de
[5] Department of Neuroradiology, University Hospital of Magdeburg, Leipziger Str. 44, 39120 Magdeburg, Germany. E-mail: daniel.behme@med.ovgu.de
[6] Department of Healthcare Telematics and Medical Engineering, University of Magdeburg, Universitätsplatz 2, 39106 Magdeburg, Germany. E-mail: philipp.berg@ovgu.de
[7] Laboratory of Fluid Dynamics and Technical Flows, University of Magdeburg, Universitätsplatz 2, 39106 Magdeburg, Germany. E-mail: samuel.voss@ovgu.de
[8] Forschungscampus STIMULATE, University of Magdeburg, Universitätsplatz 2, 39106 Magdeburg, Germany.

ABSTRACT

The treatment of intracranial aneurysms (IAs) with flow diverters (FD) has become an established minimally-invasive intervention, showing particularly high rates of complete aneurysm occlusion, especially in the case of sidewall aneurysms. The role of FD in treating bifurcation IAs is still under discussion, as some aneurysms show no long-term improvement. This study aims to explore potential hemodynamic factors contributing to unsuccessful treatment outcome by analyzing retrospective data, with the goal of predicting the success of FD treatment. Twelve intracranial media bifurcation aneurysms patients treated with a state-of-the art FD device are included. Successful treatment was observed in six patients, whereas the other six showed no IA occlusion after follow-up. Patient-specific surface models are extracted based on pre-interventional 3D digital subtraction angiography followed by a morphologic analysis. Post-interventional treatment stages are virtually created using an in-house fast virtual stenting approach. Image-based blood flow simulations compare hemodynamics before and after intervention in successful and unsuccessful treatments. Reductions in all flow-related parameters induced by the FD are observed, regardless of the treatment outcome. IAs with unsuccessful treatment outcome show tendencies to higher morphological parameters, extreme hemodynamic values, and increased stent shear stress. However, these findings suggest that the hemodynamic and morphological results alone do not accurately predict the outcome.

Keywords: cerebral blood flow, CFD, endovascular treatment, flow diverter, hemodynamics, intracranial aneurysms

NOMENCLATURE

AV	$[m/s]$	averaged velocity
$AWSS$	$[Pa]$	averaged wall shear stress
NIR	$[kg/s]$	neck inflow rate
PI	$[-]$	pulsatility index
SSS	$[Pa]$	stent shear stress

1. INTRODUCTION

Intracranial aneurysms (IAs) are pathological vascular dilatations in the cerebral arteries, with a prevalence of 2 to 5 % in adults [1]. 22 % of IAs are localized at the middle cerebral artery (MCA) [2]. In recent years, endovascular treatment methods have become increasingly popular, allowing IAs to be treated in a minimally invasive procedure [3]. In addition to (stent-assisted) coiling, the deployment of a flow diverter (FD) became an established treatment option. The FD is intended to divert the blood flow away from the IA due to its braided wires and ensure thrombosis inside the aneurysm sac, while reendothelializing the aneurysm neck [4]. In up to 76 %

of cases, this procedure results in complete occlusion of the IA [5]. However, the procedure-related morbidity and mortality is between 4 and 5 %, which highlights the importance of accurately assessing the therapy outcome [5].

FDs are particularly successful in fusiform or wide-necked IAs [6, 7]. However, the specific morphological factors that contribute to successful occlusion are still being investigated. Long et al. [8] examined the morphological parameters of small aneurysms treated with FD and observed that aneurysm sacs with branch vessels or a larger aneurysm diameter make occlusion more difficult. The success of a FD for bifurcation aneurysms is also under discussion, as problems can occur due to occlusion of the neighboring vessels [9, 6, 7].

Numerical blood flow simulations and virtual stenting of the FD can be performed to investigate the hemodynamic influence of a FD. There are numerous fast virtual stenting methods and also several studies in which the influence of a FD on hemodynamics is investigated using this method [10]. Larrabide et al. [11] investigated the hemodynamic changes caused by the FD in internal carotid artery (ICA) aneurysms using a fast virtual stent placement method. A significant reduction in wall shear stress (WSS) and velocity is observed. Additionally, the shape of the aneurysms was considered, showing greater reductions in fusiform aneurysms compared to saccular aneurysms. Cebral et al. [12] and Levitt et al. [13] also followed a similar approach in their study. Both studies also demonstrate a significant reduction in flow into the aneurysm dome and in WSS on the aneurysmal wall following FD treatment. These studies suggest that morphological and hemodynamic parameters can be linked to treatment success. However, it is not possible to determine exactly which conditions lead to good occlusion of an IA.

In this study, the focus is on MCA aneurysms. Their localization at a bifurcation poses a particular challenge for flow diversion. The FD necessarily covers one of the two main branches. Therefore, by performing a retrospective analysis this study examines whether the previous results on the relation between morphological and hemodynamic parameters and treatment outcome can be transferred to bifurcation aneurysms.

2. MATERIALS AND METHODS

Figure 1 illustrates the study workflow. Initially, digital subtraction angiography (DSA) is performed pre-interventionally. The vessels are segmented and converted to a 3D vessel model. This model serves as a basis for morphological analysis. Subsequently, a FD is virtually deployed in the model, and numerical blood flow simulations are carried out for both the pre-stented and stented models.

2.1. Patient data

The study contains the retrospective data of 11 patients and includes 12 aneurysms located at the MCA-bifurcation. All patients were treated with the p48 MW Flow Modulation Device (phenox, Bochum Germany) at Leipzig University Hospital. After the procedure, all cases were evaluated using the O'Kelly-Marotta (OKM) [14] and Saatci-Cekrige (SCS) [15] scores, which help to determine the success of the procedure. Based on the scores, this cohort includes six cases in which the aneurysm occlusion is achieved. These cases are referred to as successful in the following. In six cases, incomplete occlusion occurs, these cases are labeled as unsuccessful. An overview of the patient data is provided in Table 1.

Table 1. Overview of the therapeutic success of patient cases using classification by the O'Kelly-Marotta (OKM) and Saatci-Cekrige score (SCS).

Case	OKM	SCS	Success
1	D	1c	yes
2	C1	1c	yes
3	A1	3	no
4	D	1c	yes
5	A1	3	no
6	A1	3	no
7	A1	3	no
8	A1	3	no
9	D	1c	yes
10	D	1c	yes
11	A1	3	no
12	C2	5	yes

2.2. Image acquisition

All endovascular treatments are performed using Philips Allura Xper Biplane AngioSuite (Philipps Medical Systems DMC GmbH, Hamburg, Germany). The procedures and image acquisitions were conducted between January 2018 and December 2023. A monoplanar 3D rotational angiography (3D-RA) is performed with a rotation time of 4 s. A manual injection of 20 ml of contrast medium (Imeron 300, Bracco Imaging GmbH, Konstanz, Germany) is administered during the procedure. The pre-interventional 2D images are acquired shortly before FD deployment. Isotropic voxel sizes is 0.27 mm for all acquisitions.

2.3. Image segmentation

The extraction of patient-specific vascular structures from the 3D DSA data was performed using MeVisLab v3.4.1 (MeVis Medical Solutions AG, Bremen, Germany). To obtain the initial segmentation, threshold-based methods combined with global Laplacian smoothing were employed. Following the segmentation process, the resulting mask was converted into a triangulated 3D surface mesh utiliz-

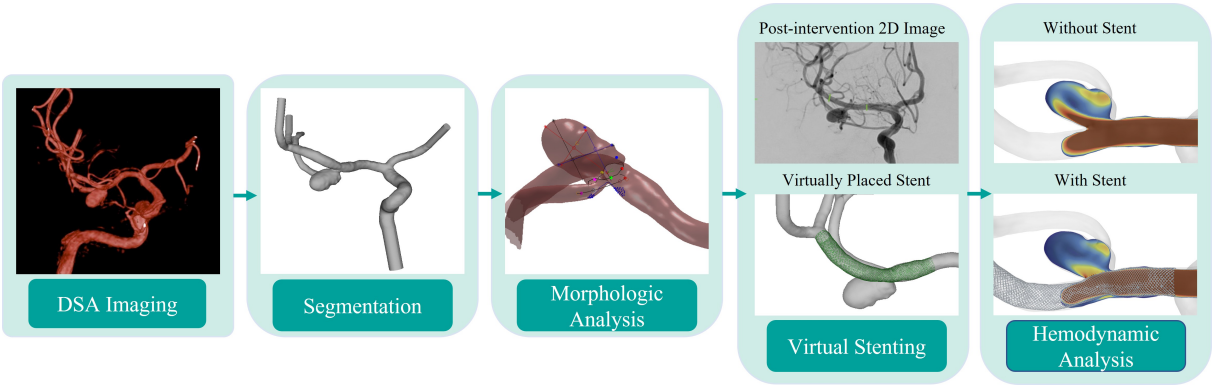

Figure 1. The workflow includes medical imaging, vessel segmentation, and morphological analysis of the extracted 3D vessel model. This is followed by virtual FD placement and a final hemodynamic analysis through numerical blood flow simulations for both pre-stented and stented models.

ing the marching cubes algorithm. For the post-processing of the segmentation the open-source 3D creation suite Blender v2.9 (BlenderFoundations, Amsterdam, Netherlands) is used. The steps performed with this software are the manual removal of artifacts, separating incorrectly fused vessel sections, extrusion of the in- and outlet cross-sections perpendicular to the vessel axis and optimizing the triangulated mesh. A total of 12 pre-interventional patient-specific models are extracted from the 3D DSA data. As shown in Figure 1, these models are used for in house fast virtual stenting approach.

2.4. Fast virtual stenting approach

The virtual FD geometries are created using an in house fast virtual stenting approach. This software is employed to virtually place the FD in patient-specific vascular models [16]. The exact position of the FD within the vessel is determined based on 2D images taken after the intervention. The FD is precisely positioned to match its placement during the initial procedure. The stent lengths and diameters used in the procedure are known and are therefore adapted to the size of the virtual stent. Stent diameters of 2 and 3 mm are used and the stent length varies between 9 and 18 mm.

2.5. Morphologic parameters

The morphologic parameters are calculated using Saalfelds et al. [17] semiautomatic neck curve reconstruction tool. This approach requires a vessel centerline, which is extracted using the VMTK v1.4.0 (Vascular Modeling Toolkit, vmtk.org) software. The morphological parameters investigated are the aneurysm area, the aneurysm volume, the orthogonal height (H_{ortho}) and the aspect ratio. The aspect ratio results from the orthogonal height divided by the maximum distance between two points on the neck curve. Furthermore, with regard to morphology, the 2D images before and after the intervention are qualitatively analyzed to identify possible changes in morphology due to the treatment.

2.6. Hemodynamic simulation and analysis

To analyze the hemodynamic differences before and after FD deployment, numerical blood flow simulations are performed using the finite-volume solver STAR-CCM+ v17.06 (Siemens PLM Software Inc., Plano, TX, USA) following the guidelines by Berg et al. [18]. The IA models were spatially discretized using polyhedral cells with a maximum base size of 0.07 mm, along with five layers of prism cells to ensure accurate resolution of near-wall flow. In order to accurately capture the individual stent struts, the discretization around the FD is refined using a base size of 0.016 mm. (A comparison with a refined 0.0094 mm mesh was conducted, showing a deviation of less than 1 % in the results. Therefore, the 0.016 mm base size was maintained.) These settings result in a total number of cells between 2.5 and 4.8 million for configurations without a FD and between 10.6 and 22.7 million for configurations with a FD, respectively. Inlet and outlet boundary conditions must be defined for the hemodynamic simulations as no patient-specific data is available. For the inlet, a representative inflow curve was taken from Cebral et al. [12]. For configurations without a stent, area-weighted outflow splitting was employed to ensure physiologically appropriate flow distribution across outlets [19]. The resulting time-dependent pressure waveforms were then used as outflow boundary conditions in the corresponding stented configurations, thereby enabling flow redistribution induced by the FD. All vessel walls were modeled as rigid and with no-slip wall condition. Blood is simplified as a fluid with incompressible ($\rho = 1056\ \mathrm{kg/m^3}$) and non-Newtonian properties (Carreau-Yasuda model parameters taken from Robertson et al. [20]). The Reynolds number in the modeled geometries did not exceed 1000. Therefore, laminar flow conditions were assumed for all simulations. Two cardiac cycles are simulated for each of the 24 configurations. The first cycle is used for initialization and the second cycle is used for the actual

hemodynamic evaluation.

Analyzed hemodynamic parameters are the

- Average Velocity inside the aneurysm sac (AV)
- Neck Inflow Rate (NIR): The net flow rate entering the aneurysm through the ostium. [21]
- Pulsatility Index regarding NIR (PI_NIR): PI quantifies the amplitude of NIR along the cardiac cycle in relation to the mean NIR [11].
- Average Wall Shear Stress (AWSS): The AWSS describes the tangential shear stress along the vessel wall over one cardiac cycle.
- Pulsatility Index regarding WSS (PI_WSS): PI quantifies the amplitude of WSS along the cardiac cycle in relation to the mean WSS [11].
- Stent Shear Stress (SSS): The time-averaged SSS describes the tangential shear stress along the stent over one cardiac cycle [22].

3. RESULTS

3.1. Morphologic analysis

The comparison of the morphologic parameters for the pre-interventional geometries is presented in Table 2. It can be observed that all morphologic parameters are higher in the unsuccessful outcome category. For example, the average IA volume is 102.69 mm³ in the unsuccessful cases, while it is 83.57 mm³ in the successful cases. Similarly, the average IA area is 87.83 mm² in the unsuccessful cases, compared to 83.32 mm² in the successful cases.

Table 2. Results of the averaged morphological parameters of the investigated IAs in the corresponding category (successful, unsuccessful)

Parameter	Successful	Unsuccessful
IA area (mm^2)	83.32	87.83
IA volume (mm^3)	83.57	102.69
H_{ortho} (mm)	3.71	4.41
Aspect Ratio (-)	0.82	0.99

Further, 2D images taken before and after the procedure are compared. In certain aneurysms, vessel deformation is evident as a result of FD deployment. Figure 2 presents an example of a case where the vessel deformation induced by the FD is clearly visible. However, these morphological changes do not exhibit a direct correlation with success or unsuccessful treatment outcome.

3.2. Hemodynamic analysis

3.2.1. Quantitative evaluation

Figure 3 shows the quantitative evaluation of the peak-systolic intra-aneurysmal blood flow velocity for two selected cases, representing successful and unsuccessful FD treatment outcome. In both cases, the blood flow in the aneurysm dome is visualized

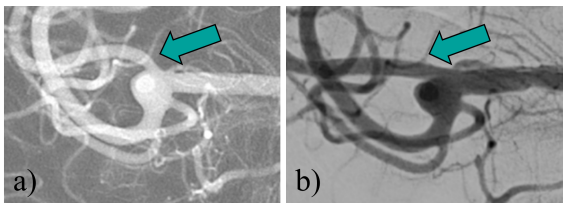

Figure 2. Representative case showing FD-induced vessel deformation; a) before intervention and b) after FD depolyment.

before and after FD deployment. It is evident that the deployment of the virtual FD leads to a reduction in the intra-aneurysmal blood flow velocity in both cases. The direct comparison shows that the reduction is even higher in the unsuccessful outcome than in the successful one. This observation can be confirmed by other cases.

The SSS is presented in Figure 4, with one successful and one unsuccessful case selected as examples. Each case is shown from two different perspectives to enable a more detailed analysis. In Figure 4a), the stent is visible from within the aneurysm, while in Figure 4b), it can be observed from the ostium into the aneurysm. In perspective a), no clear differences in the distribution of the SSS between the successful and unsuccessful cases are noticed. However, this is considerably different for perspective b). In both cases, increased SSS values can be detected near the aneurysm neck region. In the unsuccessful outcome, the SSS on the inside of the stent is notably increased, being more than four times larger. This tendency can be confirmed by the other cases.

3.2.2. Qualitative evaluation

The bar chart in Figure 5 presents the mean relative changes in hemodynamic parameters, categorized into successful and unsuccessful outcome. It can be observed that all parameters exhibit the same pattern of relative changes, with both positive and negative trends being consistent across all cases, regardless of the treatment outcome. For instance, there are negative relative changes in the values for velocity, NIR and AWSS. The parameters related to pulsatility show positive changes in the values. The greatest AWSS reduction (-54.4 %) occurs in unsuccessful cases, compared to -42.8 % in successful ones. AWSS pulsatility increases more in unsuccessful outcomes (36.7 %) than in successful (25.5 %). The largest intergroup difference is in NIR, with a 12.6 % greater reduction in the unsuccessful group.

Finally, Figure 6 presents the absolute values of all selected parameters and analyzed cases before and after FD deployment. Consistent with the observations of relative changes, a reduction in velocity, AWSS, and NIR values are evident following FD placement. The absolute values of the pulsatility regarding AWSS and NIR increase. Additionally, the analysis of absolute values reveals that ex-

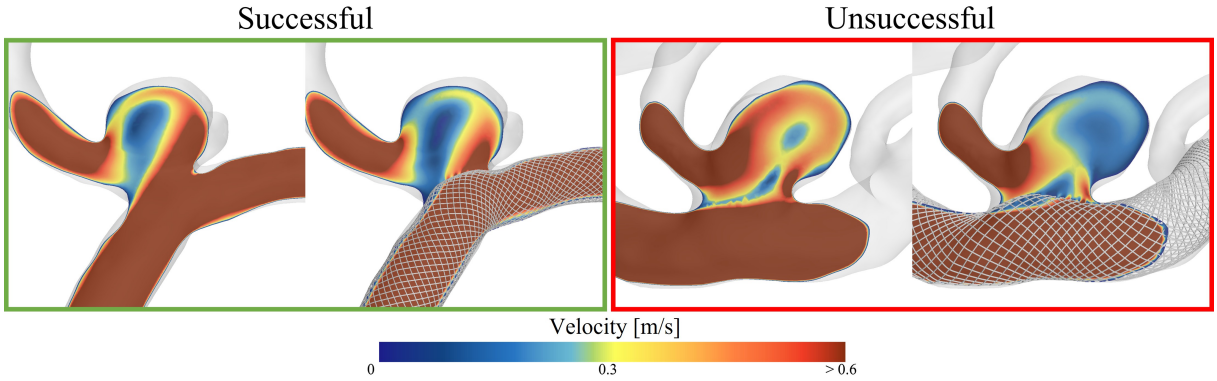

Figure 3. Visualisation of the peak-systolic intra-aneurysmal blood flow velocity before and after virtual stent deployment for a successful case and an unsuccessful case.

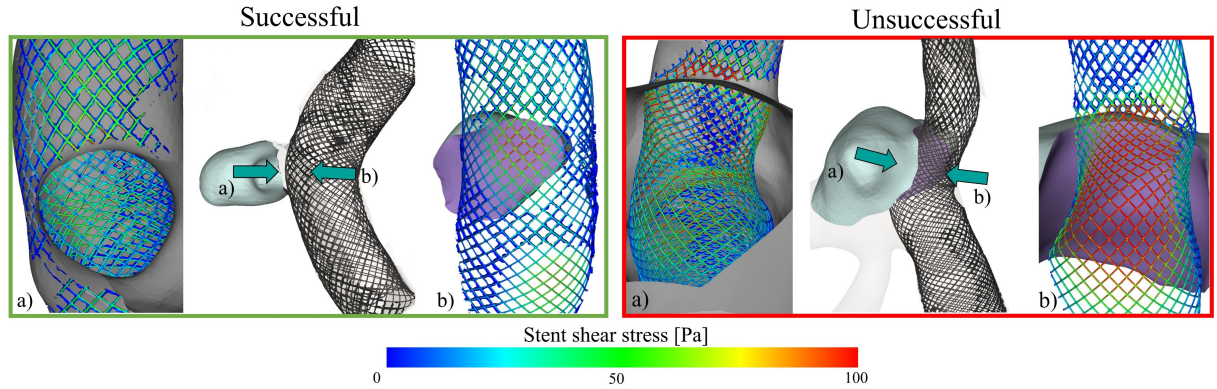

Figure 4. Visualisation of the SSS for a successful and unsuccessful case from two different perspectives. The arrows show the indicated direction of view (a) perspective from the aneurysm dome on the FD, b) perspective on the ostium of the aneurysm).

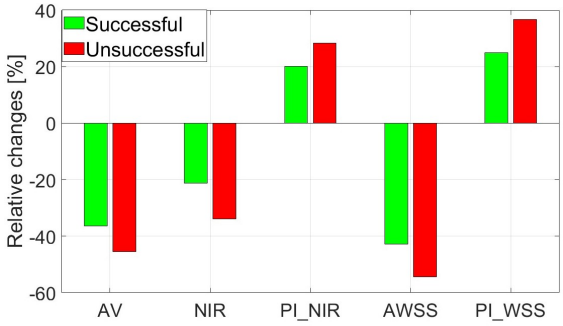

Figure 5. Mean relative changes in AV, NIR, PI_NIR, AWSS, and PI_WSS before and after FD deployment, categorized into successful and unsuccessful outcome.

treme values often occur in unsuccessful treatment outcomes. This is particularly noticeable in the pre-interventional AWSS values, which range from 1.7 to 12.2 Pa. In contrast, for successful cases, the maximum AWSS value is 5.62 Pa, while the minimum is 3.09 Pa.

4. DISCUSSION

The results of the morphological analysis indicate a tendency for FD therapy to be less successful in larger MCA aneurysms. However, no specific parameter or associated threshold can be identified that reliably predicts the success of FD deployment in relation to morphological characteristics. Consequently, the analysis of the morphological parameters of IAs alone does not provide a clear classification of whether the use of a FD will lead to full occlusion of the IA.

The 2D comparison of the images before and after treatment demonstrates, that in some cases there are morphological deformation of the vessels due to the FD. This often appears as a straightening of the surrounding vessels. Even if it is not clearly identifiable whether this deformation has a positive or negative influence on the treatment success, it could make a difference for the subsequent hemodynamic analysis. Voß et al. [23] investigated the effect of vessel deformation on MCA aneurysms and showed that these morphological changes impact intra-aneurysmal hemodynamics. To achieve this, they analyzed 3DRA data collected before and after FD treatment. In this work, only 2D images

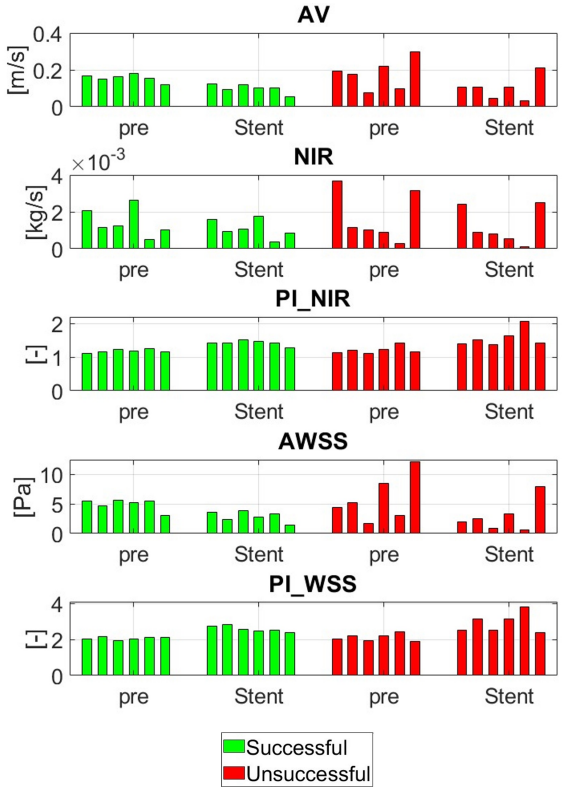

Figure 6. Absolute values of the parameters AV, NIR, PI_NIR, AWSS, and PI_WSS before and after FD deployment, divided into successful and unsuccessful outcome.

after treatment are available. To enable a more comprehensive analysis of the precise morphological and hemodynamic conditions following FD treatment, it would be beneficial for subsequent studies to include post-interventional 3D images. This would provide a more realistic representation of the morphology and stent placement and thus also improve the hemodynamic analysis.

FD deployment aims to occlude the aneurysm and prevent rupture. Two effects play a decisive role in its success. Firstly, thrombus formation in the aneurysm and secondly, endothelization along the FD and the neck of the aneurysm [4].

The FD-induced reduction of blood AV inside the aneurysm, the NIR and the AWSS is expected and confirmed by the presented results. These findings agree with previous studies by Thormann et al. [24] and Kulcsár et al. [25]. It is noticeable that the pulsatility of both the NIR and the WSS increase after FD deployment, independent of the occlusion state. This behavior is also identified in the study by Larrabide et al. [11] who investigated the hemodynamic effects of a FD in a similar study design.

However, it is unexpected that the average reduction of these parameters is greater in the unsuccessful cases in both absolute and relative values. As also stated by Ravindran et al. [4], especially the reduced velocity is a key factor for thrombus formation and thus for occlusion of the aneurysm. These results therefore do not contribute to differentiating between successful and unsuccessful cases.

The study by Mut et al. [26] has a similar design and investigates potential causes for fast or slow aneurysm occlusion following FD treatment. In contrast to the present results, this study identified significant differences regarding AV and NIR. Both were found to be significantly lower in cases with fast occlusion. The key difference is the focus on IAs located at the ICA and posterior communicating artery (PCOM), rather than MCA-bifurcation aneurysms. The results of the present study suggest that Mut et al.'s findings may not be applicable to MCA-bifurcation aneurysms, requiring further analysis of hemodynamic parameters.

Further, the absolute values are analyzed in order to possibly predict the outcome success using hemodynamic analysis. It is noticeable that the unsuccessful cases often represent minimum or maximum values, see Figure 6. This could indicate abnormal flow conditions that could prevent the aneurysm occlusion mechanisms introduced above. Regarding the instability assessment of IAs, abnormal flow is considered as critical factor [27]. Notably, a trend towards abnormal flow conditions or extreme hemodynamic parameters is already visible in the pre-interventional simulations of the unsuccessful cases. Therefore, such an indicator might be used pre-interventionally to assess the success of FD treatment.

In addition, SSS is evaluated. Berg et al. [22] found that an increased SSS is present in regions where endothelialization did not occur. At lower SSS, endothelial proliferation was seen both on the stented parent artery and on the open segments of the stent. Accordingly, this study highlights increased SSS in the unsuccessful cases. This could therefore lead to reduced endothelialization and serve as an explanation for incomplete aneurysm occlusion. Further studies should investigate this in more detail.

Limitations The first limitation is the small cohort size of 12 MCA IAs, with only six in each successful and unsuccessful group. A larger cohort and the consideration of all OKM score classes would provide more precise information on the hemodynamic effects of FD deployment.

Another limitation is the uncertainty caused by the segmentation and manual processing steps involved in creating the patient-specific geometries. This can lead to discrepancies from the original shape of the vessel. However, comparing the medical images and the 3D models was utilized to reduce 3D model uncertainty.

Some simplifications are necessary for the hemodynamic simulations. These include the simplification of the fluid properties of blood as well as a simplified representation of the wall and the inlet and outlet conditions. In this study, it would be of

special interest to apply patient-specific inlet conditions. Unfortunately, patient-specific flow rates are rarely available, but they could make a difference in estimating the success of therapy [28].

Additionally, it should be considered to adopt a more multifactorial approach by incorporating additional patient-specific factors into the prediction of treatment success. This could include diseases such as hypertension, as well as lifestyle factors like smoking. These factors were not considered in the current approach, which focused solely on morphology and hemodynamics. Furthermore, the morphological analysis could be extended, allowing a more detailed analysis of the aneurysm's surroundings and the position of the side branches.

Moreover, the availability of both 2D and 3D DSA images after the intervention would be highly advantageous. This would enable a more accurate assessment of vessel deformation and allow for a more realistic placement of the virtual FD.

5. CONCLUSION

This study addresses the morphological and hemodynamic analysis of MCA-bifurcation aneurysms to evaluate the treatment success of FD deployments. The findings indicate that larger IAs are more likely to experience unsuccessful treatment outcome, and the hemodynamic parameters in these cases show a greater relative change compared to successful cases. Abnormal flow conditions in the unsuccessful cases, along with higher SSS, could delay occlusion. This pilot study represents a first step toward identifying specific parameters for predicting treatment success for MCA aneurysm. While hemodynamic and morphological analysis alone may not be sufficient, these findings highlight the need for a multifactorial approach.

ACKNOWLEDGEMENTS

This study was partly funded by the Federal Ministry of Education and Research in Germany within the Forschungscampus STIMULATE (grant number 13GW0473A and 13GW0674C) and the German Research Foundation (grant number 548907942).

REFERENCES

[1] Xu, Z., Rui, Y.-N., Hagan, J. P., and Kim, D. H., 2019, "Intracranial aneurysms: pathology, genetics, and molecular mechanisms", *NeuroMolecular Medicine*, Vol. 21 (4), pp. 325–343.

[2] Keedy, A., 2006, "An overview of intracranial aneurysms", *McGill Journal of Medicine: MJM*, Vol. 9 (2), p. 141.

[3] Lee, K. S., Zhang, J. J., Nguyen, V., Han, J., Johnson, J. N., Kirollos, R., and Teo, M., 2022, "The evolution of intracranial aneurysm treatment techniques and future directions", *Neurosurgical Review*, Vol. 45 (1), pp. 1–25.

[4] Ravindran, K., Casabella, A. M., Cebral, J., Brinjikji, W., Kallmes, D. F., and Kadirvel, R., 2020, "Mechanism of action and biology of flow diverters in the treatment of intracranial aneurysms", *Neurosurgery*, Vol. 86 (Supplement_1), pp. S13–S19.

[5] Brinjikji, W., Murad, M. H., Lanzino, G., Cloft, H. J., and Kallmes, D. F., 2013, "Endovascular treatment of intracranial aneurysms with flow diverters: a meta-analysis", *Stroke*, Vol. 44 (2), pp. 442–447.

[6] Topcuoglu, O. M., Akgul, E., Daglioglu, E., Topcuoglu, E. D., Peker, A., Akmangit, I., Belen, D., and Arat, A., 2016, "Flow diversion in middle cerebral artery aneurysms: is it really an all-purpose treatment?", *World Neurosurgery*, Vol. 87, pp. 317–327.

[7] Michelozzi, C., Darcourt, J., Guenego, A., Januel, A.-C., Tall, P., Gawlitza, M., Bonneville, F., and Cognard, C., 2018, "Flow diversion treatment of complex bifurcation aneurysms beyond the circle of Willis: complications, aneurysm sac occlusion, reabsorption, recurrence, and jailed branch modification at follow-up", *Journal of Neurosurgery*, Vol. 131 (6), pp. 1751–1762.

[8] Long, S., Shi, S., Tian, Q., Wei, Z., Ma, J., Wang, Y., Yang, J., Han, X., and Li, T., 2024, "Correlation of flow diverter malapposition at the aneurysm neck with incomplete aneurysm occlusion in patients with small intracranial aneurysms: a single-center experience", *American Journal of Neuroradiology*, Vol. 45 (1), pp. 16–21.

[9] Gawlitza, M., Januel, A.-C., Tall, P., Bonneville, F., and Cognard, C., 2016, "Flow diversion treatment of complex bifurcation aneurysms beyond the circle of Willis: a single-center series with special emphasis on covered cortical branches and perforating arteries", *Journal of NeuroInterventional Surgery*, Vol. 8 (5), pp. 481–487.

[10] Stahl, J., Marsh, L. M. M., Thormann, M., Ding, A., Saalfeld, S., Behme, D., and Berg, P., 2023, "Assessment of the flow-diverter efficacy for intracranial aneurysm treatment considering pre-and post-interventional hemodynamics", *Computers in Biology and Medicine*, Vol. 156, p. 106720.

[11] Larrabide, I., Geers, A. J., Morales, H. G., Bijlenga, P., and Rüfenacht, D. A., 2016, "Change in aneurysmal flow pulsatility after flow diverter treatment", *Computerized Medical Imaging and Graphics*, Vol. 50, pp. 2–8.

[12] Cebral, J., Mut, F., Raschi, M., Scrivano, E., Ceratto, R., Lylyk, P., and Putman, C., 2011, "Aneurysm rupture following treatment with flow-diverting stents: computational hemodynamics analysis of treatment", *American Journal of Neuroradiology*, Vol. 32 (1), pp. 27–33.

[13] Levitt, M. R., McGah, P. M., Aliseda, A., Mourad, P. D., Nerva, J. D., Vaidya, S. S., Morton, R. P., Ghodke, B. V., and Kim, L. J., 2014, "Cerebral aneurysms treated with flow-diverting stents: computational models with intravascular blood flow measurements", *American Journal of Neuroradiology*, Vol. 35 (1), pp. 143–148.

[14] O'Kelly, C., Krings, T., Fiorella, D., and Marotta, T., 2010, "A novel grading scale for the angiographic assessment of intracranial aneurysms treated using flow diverting stents", *Interventional Neuroradiology*, Vol. 16 (2), pp. 133–137.

[15] Cekirge, H., and Saatci, I., 2016, "A new aneurysm occlusion classification after the impact of flow modification", *American Journal of Neuroradiology*, Vol. 37 (1), pp. 19–24.

[16] Berg, P., Daróczy, L., and Janiga, G., 2017, "Virtual stenting for intracranial aneurysms: A risk-free, patient-specific treatment planning support for neuroradiologists and neurosurgeons", *Computing and Visualization for Intravascular Imaging and Computer-Assisted Stenting*, Elsevier, pp. 371–411.

[17] Saalfeld, S., Berg, P., Niemann, A., Luz, M., Preim, B., and Beuing, O., 2018, "Semiautomatic neck curve reconstruction for intracranial aneurysm rupture risk assessment based on morphological parameters", *International Journal of Computer Assisted Radiology and Surgery*, Vol. 13, pp. 1781–1793.

[18] Berg, P., Saalfeld, S., Voß, S., Beuing, O., and Janiga, G., 2019, "A review on the reliability of hemodynamic modeling in intracranial aneurysms: why computational fluid dynamics alone cannot solve the equation", *Neurosurgical Focus*, Vol. 47 (1), p. E15.

[19] Chnafa, C., Bouillot, P., Brina, O., Delattre, B., Vargas, M., Lovblad, K., Pereira, V., and Steinman, D., 2017, "Vessel calibre and flow splitting relationships at the internal carotid artery terminal bifurcation", *Physiological Measurement*, Vol. 38 (11), p. 2044.

[20] Robertson, A. M., Sequeira, A., and Owens, R. G., 2009, "Rheological models for blood", *Cardiovascular Mathematics: Modeling and Simulation of the Circulatory System*, pp. 211–241.

[21] Sugiyama, S.-i., Niizuma, K., Sato, K., Rashad, S., Kohama, M., Endo, H., Endo, T., Matsumoto, Y., Ohta, M., and Tominaga, T., 2016, "Blood flow into basilar tip aneurysms: a predictor for recanalization after coil embolization", *Stroke*, Vol. 47 (10), pp. 2541–2547.

[22] Berg, P., Iosif, C., Ponsonnard, S., Yardin, C., Janiga, G., and Mounayer, C., 2016, "Endothelialization of over-and undersized flow-diverter stents at covered vessel side branches: an in vivo and in silico study", *Journal of Biomechanics*, Vol. 49 (1), pp. 4–12.

[23] Voss, S., Beuing, O., Janiga, G., and Berg, P., 2019, "Stent-induced vessel deformation after intracranial aneurysm treatment–A hemodynamic pilot study", *Computers in Biology and Medicine*, Vol. 111, p. 103338.

[24] Thormann, M., Stahl, J., Marsh, L., Saalfeld, S., Sillis, N., Ding, A., Mpotsaris, A., Berg, P., and Behme, D., 2024, "Computational Flow Diverter Implantation—A Comparative Study on Pre-Interventional Simulation and Post-Interventional Device Positioning for a Novel Blood Flow Modulator", *Fluids*, Vol. 9 (3), p. 55.

[25] Kulcsár, Z., Augsburger, L., Reymond, P., Pereira, V. M., Hirsch, S., Mallik, A. S., Millar, J., Wetzel, S. G., Wanke, I., and Rüfenacht, D. A., 2012, "Flow diversion treatment: intra-aneurismal blood flow velocity and WSS reduction are parameters to predict aneurysm thrombosis", *Acta Neurochirurgica*, Vol. 154, pp. 1827–1834.

[26] Mut, F., Raschi, M., Scrivano, E., Bleise, C., Chudyk, J., Ceratto, R., Lylyk, P., and Cebral, J. R., 2015, "Association between hemodynamic conditions and occlusion times after flow diversion in cerebral aneurysms", *Journal of NeuroInterventional Surgery*, Vol. 7 (4), pp. 286–290.

[27] Rayz, V. L., and Cohen-Gadol, A. A., 2020, "Hemodynamics of cerebral aneurysms: Connecting medical imaging and biomechanical analysis", *Annual Review of Biomedical Engineering*, Vol. 22 (1), pp. 231–256.

[28] Voß, S., Niemann, U., Saalfeld, S., Janiga, G., and Berg, P., 2025, "Impact of workflow variability on image-based intracranial aneurysm hemodynamics", *Computers in Biology and Medicine*, Vol. 190, p. 110018.